Research Article

Journal of Environmental Nanotechnology

Enhanced Photoelectrochemical Water Splitting Performance of Titania Nanotubes by Anodization

G. P. Jeslin Jebish* and R. P. Jebin

Department of Physics and Research Centre, Muslim Arts College (Affiliated to Manonmanium Sundaranar University), Thiruvithancode, TN, India

Received: 15.04.2025 Accepted: 11.05.2025 Published: 30.06.2025

*jeslinjebish12@gmail.com

ABSTRACT

This study examines the effect of anodization voltage (12 V, 20 V, 30 V) on the electrochemical characteristics of TiO_2 nanotubes for photoelectrochemical water splitting applications. Our findings indicate that elevated anodization voltages (30 V) result in TiO_2 nanotubes with markedly diminished charge transfer resistance (625 Ω) and improved photoconversion efficiency (1.42%) relative to lower voltages. Electrochemical impedance spectroscopy verifies a linear correlation between anodization voltage and barrier layer thickness of roughly 0.8 nm/V, while also exhibiting enhanced electron transport properties for the 30 V samples. The results identify anodization voltage as a critical factor for enhancing TiO_2 nanotube efficacy in sustainable hydrogen production systems. This study enhances the fundamental comprehension of the influence of electrochemical anodization parameters on the characteristics and efficacy of TiO_2 nanotubes, offering critical insights for the systematic design and optimization of effective photoanodes for sustainable hydrogen production *via* solar water splitting.

Keywords: Titania nanotubes; Electrochemical impedance spectroscopy; Photocurrent density; Photoconversion efficiency.

1. INTRODUCTION

The global energy challenge and environmental issues associated with fossil fuel use have led to significant research on clean, renewable energy sources. Hydrogen serves as a versatile and environmentally advantageous energy carrier, offering the potential for a more prosperous and sustainable future (Gabov and Lizikova, 2022). Photoelectrochemical (PEC) water splitting is one of the various hydrogen generation processes that offers a sustainable method for converting solar energy directly into chemical energy (Mishra *et al.* 2007) Titanium dioxide (TiO_2) is a widely researched photoanode material for photoelectrochemical (PEC) water splitting, attributed to its stability, non-toxicity, corrosion resistance, and suitable band edge positions (Song *et al.* 2022). The findings of this study may enhance the understanding and optimization of TiO_2 nanotube-based photoanodes, resulting in more efficient and sustainable solar water-splitting systems.

Despite these advantages, the practical application of TiO_2 in solar water splitting is constrained by its wide bandgap (approximately 3.2 eV), which restricts light absorption mainly to the ultraviolet region, and its comparatively high recombination rate of photogenerated charge carriers (Rathod and Waghuley, 2015). Nanostructuring of TiO_2 has been investigated as a strategy to improve its photoelectrochemical performance, addressing existing limitations (Schulte *et al.* 2010). One-dimensional TiO_2 nanotubes have attracted considerable interest among various nanostructures due to their distinctive properties, such as a high specific surface area, directional charge transport along the tube axis, and adjustable dimensions (Rafique *et al.* 2023).

Electrochemical anodization is a versatile method for the fabrication of highly ordered TiO_2 nanotube arrays, allowing for precise control over their morphology and dimensions. The anodization process entails the oxidation of titanium metal within a fluoride-containing electrolyte while applying an electric voltage (Zakir *et al.* 2020). The mechanism of nanotube formation involves a dynamic equilibrium between the processes of oxide layer formation and dissolution, influenced by several parameters such as applied voltage, electrolyte composition, temperature, and the duration of anodization (Lettieri *et al.* 2021).

The applied voltage during anodization significantly influences the morphology, growth rate, and electrochemical properties of the resulting TiO_2 nanotubes (Roy *et al.* 2011). Increased anodization voltages generally lead to larger nanotube diameters, lengths, and wall thicknesses, which subsequently affect their optical absorption, charge transport characteristics, and overall photoelectrochemical performance. Nevertheless, the relationship between anodization voltage and the resulting electrochemical impedance characteristics, which influence charge transport and

transfer processes, remains unclear (Meena *et al.* 2022). Electrochemical impedance spectroscopy (EIS) serves as an effective method for examining the electronic and ionic processes at the electrode-electrolyte interface. Analyzing the impedance response of TiO_2 nanotubes across different frequencies provides insights into charge transfer resistance, space charge layer capacitance, and electron transport. The parameters are crucial for understanding and improving the photoelectrochemical performance of TiO_2 nanotubes in water-splitting applications (David *et al.* 2018).

This study examines the influence of anodization voltage (12 V, 20 V, and 30 V) on the morphology, crystal structure, electrochemical impedance characteristics, and photoelectrochemical water splitting performance of TiO_2 nanotubes. This research aims to elucidate the relationships among anodization voltage, electrochemical properties, and photoelectrochemical performance, thereby offering insights for the design and optimization of TiO_2 nanotube-based photoanodes for efficient solar water splitting (Kumar *et al.* 2020).

2. MATERIALS AND METHODS

2.1 Materials

Titanium foils (99.9% purity, 0.25 mm thickness) were purchased from Sigma-Aldrich and cut into 3 × 1 cm pieces to serve as substrates for anodization. Prior to anodization, the titanium foils were sequentially cleaned with acetone, ethanol, and deionized water using an ultrasonic bath for 15 minutes in each solution to remove surface contaminants (Gong *et al.* 2001; Grimes and Mor, 2009). All chemicals used in this study, including ethylene glycol, ammonium fluoride (NH_4F), and water (H_2O), were of analytical grade and used as received without further purification.

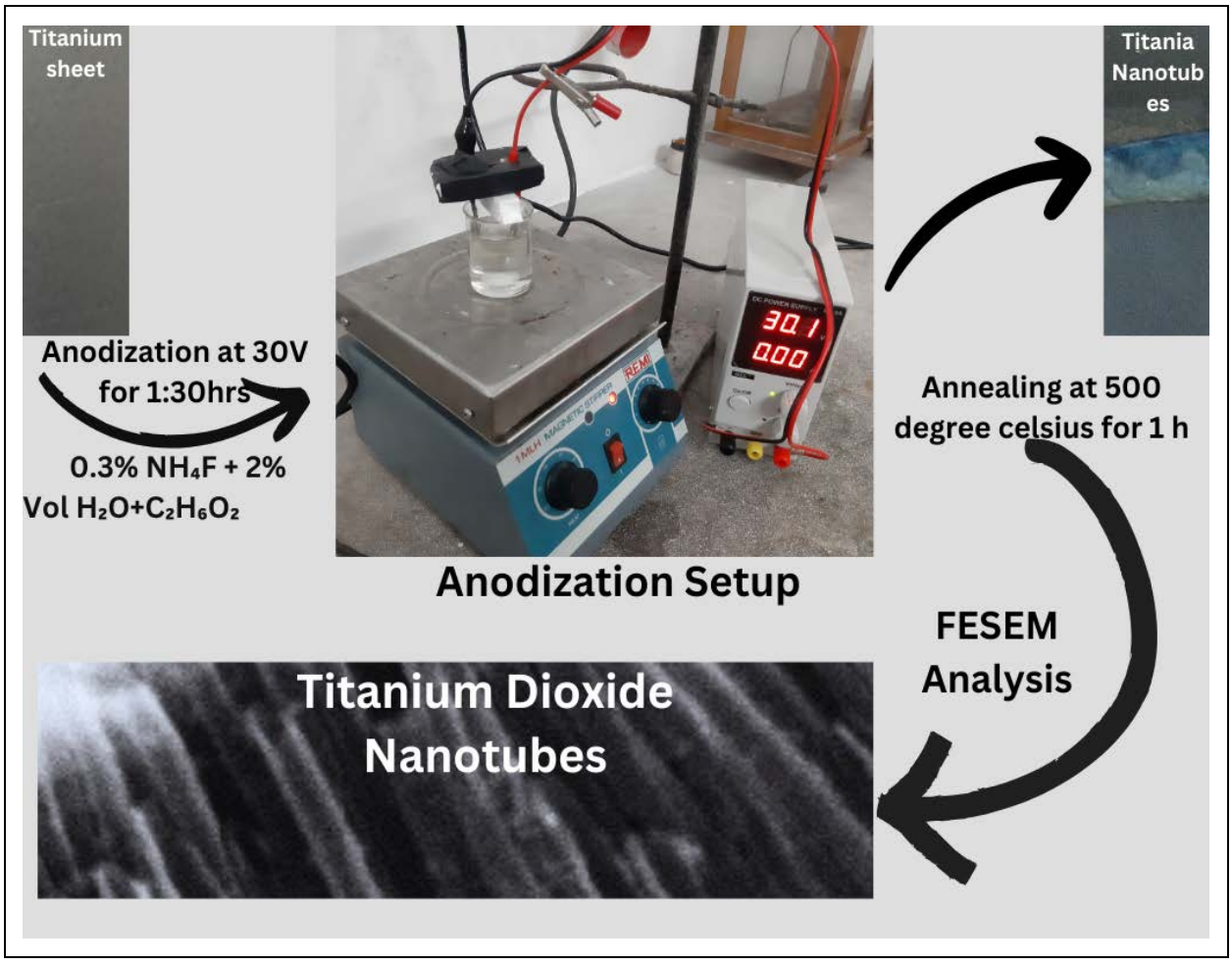


Fig. 1: Experimental setup

2.2 Fabrication of TiO_2 Nanotubes

TiO_2 nanotubes were fabricated *via* an electrochemical anodization process using a two-electrode configuration. The pre-cleaned titanium foil served as the working electrode (anode), while a platinum foil (2 cm × 2 cm) was used as the counter electrode (cathode). The electrodes were positioned

parallel to each other at a fixed distance of 2 cm to ensure a uniform electric field distribution across the titanium surface. The electrolyte solution consisted of ethylene glycol containing 0.5 M NH_4F and 2 vol% of deionized water. The anodization was performed at room temperature (25 ± 2 °C) under constant voltage conditions. Three different anodization voltages were applied: 12 V, 20 V, and 30 V, each for 90 minutes. Throughout the anodization process, the electrolyte solution was continuously stirred at 200 rpm to maintain uniform ion distribution and temperature. Fig. 1 shows the experimental setup.

After anodization, the samples were thoroughly rinsed with deionized water to remove residual electrolytes and dried under a nitrogen stream. To improve crystallinity and convert the amorphous TiO_2 to the crystalline phase, all samples were annealed in a muffle furnace at 500 °C for 2 hours in an air atmosphere, with a controlled heating and cooling rate of 2°C/min. The samples were labeled as TiO_2-12V, TiO_2-20V, and TiO_2-30V, corresponding to their respective anodization voltages.

2.3 Characterization Techniques

2.3.1 Electrochemical Impedance Spectroscopy

Electrochemical impedance spectroscopy (EIS) measurements were performed using a potentiostat/galvanostat (Autolab PGSTAT302N) in a three-electrode configuration. The TiO_2 nanotube samples served as the working electrode, a platinum wire as the counter electrode, and Ag/AgCl as the reference electrode. The measurements were conducted in a 0.1 M Na_2SO_4 electrolyte at open-circuit potential, with frequencies ranging from 100 kHz to 0.01 Hz and an AC amplitude of 10 mV.

The EIS data were analyzed using equivalent circuit modeling to extract parameters, including barrier layer resistance (R_b), charge transfer resistance (R_{ct}), and space charge layer capacitance (C_{sc}). The Mott-Schottky analysis was performed at a fixed frequency of 1 kHz to determine the flat band potential and donor density of the TiO_2 nanotubes.

2.4 Photoelectrochemical Measurements

The photoelectrochemical water splitting performance was evaluated in a quartz cell using a three-electrode configuration, with the TiO_2 nanotube samples serving as the working electrode (photoanode), a platinum wire as the counter electrode, and an Ag/AgCl reference electrode. A 1 M KOH solution (pH 13.6) served as the electrolyte. The photoanode was illuminated using a 300 W xenon lamp equipped with an AM 1.5 G filter, calibrated to provide an incident light intensity of 100 mW/cm².

Linear sweep voltammetry (LSV) was conducted in both dark and illuminated conditions at a scan rate of 10 mV/s. The photocurrent stability was assessed through chronoamperometry measurements at an applied potential of 1.23 V versus a reversible hydrogen electrode (RHE). The incident photon-to-current efficiency (IPCE) was measured at an applied potential of 1.23 V *vs*. RHE in the wavelength range of 300-600 nm.

The photoconversion efficiency (η) was calculated using the following equation:

$$\eta\% = \left[\frac{J_{Ph} \times (1.232 - V)}{P_{light}}\right] \times 100 \quad \ldots (1)$$

Where J_{ph} represents the photocurrent density (mA/cm²), V is the applied bias voltage (V vs. RHE), and P_{light} is the incident light intensity (100 mW/cm²).

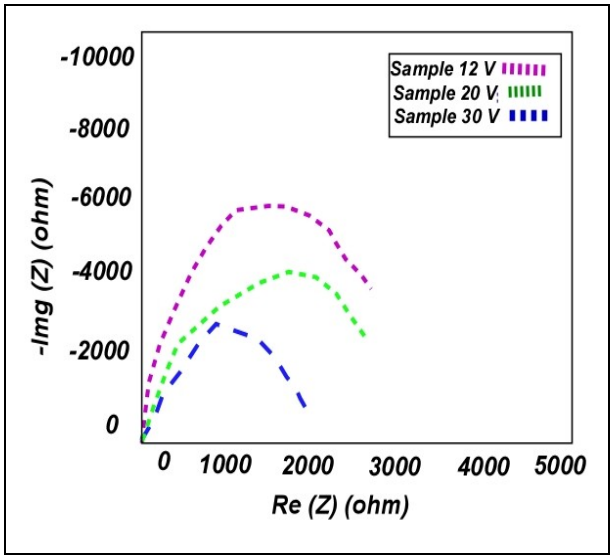


Fig. 2: Nyquist plots obtained for TiO_2-12 V, TiO_2-20 V, and TiO_2-30 V

3. RESULTS AND DISCUSSION

3.1 Electrochemical Impedance Spectroscopy Analysis

Electrochemical impedance spectroscopy was employed to investigate the electronic properties and charge transfer processes of the TiO_2 nanotubes fabricated at different anodization voltages. Fig. 2 shows the Nyquist plots obtained for TiO_2-12V, TiO_2-20V, and TiO_2-30V samples measured at open circuit potential in 0.1 M Na_2SO_4 electrolyte.

The Nyquist plots exhibited semicircles in the high-frequency region, which represent the charge transfer resistance (R_{ct}) at the electrode-electrolyte interface, followed by inclined lines in the low-frequency

region, which are associated with diffusion-limited processes. The diameter of the semicircle decreased significantly with increasing anodization voltage, indicating a reduced charge transfer resistance for samples anodized at higher voltages.

To extract quantitative information, the EIS data were fitted using an equivalent circuit model consisting of a series resistance (R_s) representing the electrolyte and contact resistance, in series with a parallel combination of charge transfer resistance (R_{ct}) and constant phase element (CPE) representing the electrode-electrolyte interface, followed by a Warburg element (W) representing diffusion processes. The fitted parameters are summarized in Table 1.

Table 1. Electrochemical parameters extracted from EIS measurements for TiO_2 nanotubes fabricated at different anodization voltages

Sample	R_s (Ω)	R_{ct} (Ω)	CPE-T (μF)	CPE-P
TiO_2-12 V	15.3	1870	22.5	0.85
TiO_2-20 V	14.8	980	35.2	0.88
TiO_2-30 V	14.2	625	48.7	0.91

The charge transfer resistance (R_{ct}) decreased dramatically from 1870 Ω for TiO_2-12V to 980 Ω for TiO_2-20V and further to 625 Ω for TiO_2-30V. This significant reduction (approximately 67%) in charge transfer resistance with increasing anodization voltage indicates enhanced charge transfer kinetics at the electrode-electrolyte interface for nanotubes fabricated at higher voltages. The improved charge transfer properties can be attributed to several factors, including:

1. Increased surface area providing more active sites for electrochemical reactions
2. Enhanced crystallinity with fewer grain boundaries, reducing trapping and recombination of charge carriers
3. Improved nanotube alignment offering more direct electron transport pathways
4. Thicker nanotube walls provide better structural stability and charge transport channels

The constant phase element (CPE) values increased with anodization voltage, reflecting the increased electrochemically active surface area of the nanotubes. The CPE-P values closer to 1 for higher anodization voltages indicate ideal capacitive behavior, suggesting a more uniform and ordered surface structure.

To gain further insights into the electronic properties of the TiO_2 nanotubes, Mott-Schottky analysis was performed at a fixed frequency of 1 kHz. Fig. 3 shows the Mott-Schottky plots ($1/C^2$ vs. potential) for the three samples. All samples exhibited positive slopes, confirming the n-type semiconductor nature of the TiO_2 nanotubes.

The flat band potential (E_{fb}) was determined from the X-axis intercept of the Mott-Schottky plot using the equation:

$$\frac{1}{C^2} = \frac{2}{e\varepsilon\varepsilon_0 N_D}\left(E - E_{fb} - \frac{kT}{e}\right) \quad \ldots (2)$$

Where C is the capacitance, e is the elementary charge, ε is the dielectric constant of TiO_2 (ε = 55), ε_0 is the permittivity of vacuum, ND is the donor density, E is the applied potential, E_{fb} is the flat band potential, k is the Boltzmann constant, and T is the absolute temperature.

The flat band potential shifted negatively with increasing anodization voltage, from -0.48 V vs. Ag/AgCl for TiO_2-12V to -0.52 V vs. Ag/AgCl for TiO_2-20V and -0.56 V vs. Ag/AgCl for TiO_2-30V. This negative shift in flat-band potential is beneficial for water oxidation, as it increases band bending at the semiconductor-electrolyte interface, thereby enhancing charge separation efficiency.

The donor density (ND), calculated from the slope of the Mott-Schottky plot, increased with anodization voltage from 5.2×10^{18} cm^{-3} for TiO_2-12V to 8.7×10^{18} cm^{-3} for TiO_2-20V and 1.3×10^{19} cm^{-3} for TiO_2-30V. The higher donor density in samples anodized at higher voltages indicates increased oxygen vacancy concentration, which can enhance the conductivity of the TiO_2 nanotubes and contribute to improved photoelectrochemical performance.

Based on the EIS data, the barrier layer thickness (d) at the bottom of the nanotubes was estimated using the equation (3): $d = \frac{\varepsilon_0 \varepsilon A}{C}$, where A is the geometrical surface area of the electrode, and C is the space charge layer capacitance at flat band potential.

The barrier layer thickness increased linearly with anodization voltage, from approximately 14 nm for TiO_2-12V to 22 nm for TiO_2-20V and 30 nm for TiO_2-30V. This linear relationship, with a proportionality constant of roughly 0.8 nm/V, is consistent with the field-assisted oxidation mechanism of titanium during anodization and provides valuable guidance for electrode design and optimization.

3.2 Photoelectrochemical Water Splitting Performance

The photoelectrochemical water splitting performance of the TiO_2 nanotubes was evaluated through linear sweep voltammetry, chronoamperometry, and incident photon-to-current efficiency measurements.

The linear sweep voltammograms of TiO_2-12V, TiO_2-20V, and TiO_2-30V samples recorded in 1 M KOH electrolyte under dark conditions and AM 1.5G illumination (100 mW/cm²) (Momeni and Ghayeb, 2015).

$TiO_2 + hv \rightarrow e^- + h^+$ reaction sequence for photoelectrochemical water splitting.

In dark conditions, all samples exhibited negligible current densities, as expected for semiconductor photoanodes. Under illumination, all samples showed substantial photocurrent, indicating successful photoelectrochemical water oxidation. The photocurrent density increased with applied potential due to enhanced band bending and improved charge separation at higher potentials (Liu *et al.* 2017).

At the standard water oxidation potential of 1.23 V versus RHE, the photocurrent densities were 0.32 mA/cm², 0.58 mA/cm², and 0.85 mA/cm² for TiO_2-12V, TiO_2-20V, and TiO_2-30V, respectively. The TiO_2-30V sample demonstrated approximately 2.7 times higher photocurrent density compared to the TiO_2-12V sample, highlighting the significant impact of anodization voltage on photoelectrochemical performance. At 30 V the nanotubes length is measured using image J software 2 micro meter is obtained.

Table 2. The photocurrent densities TiO_2 nanotubes fabricated at different anodization voltages

Samples	Voltages	Photo current densities mA/cm²
TiO_2-12 V	12 V	0.32
TiO_2-20 V	20 V	0.58
TiO_2-30 V	30 V	0.85

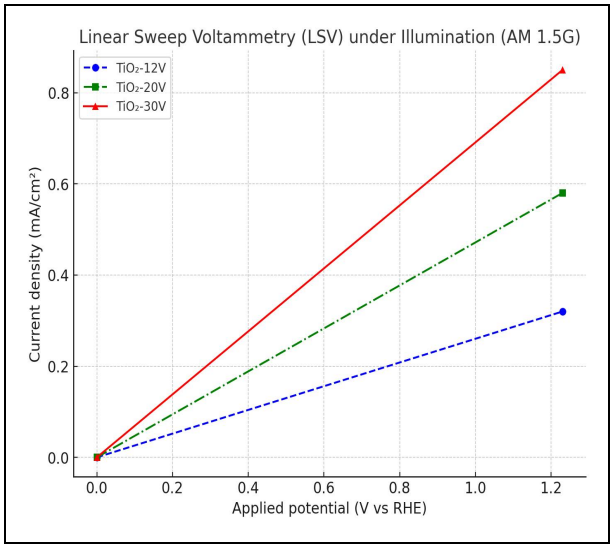


Fig. 3: A plot of potential *vs* current density

The onset potential, defined as the potential at which photocurrent begins to rise, is shifted cathodically with increasing anodization voltage. The onset potentials were approximately 0.2 V, 0.15 V, and 0.1 V versus RHE for TiO_2-12V, TiO_2-20V, and TiO_2-30V, respectively. This cathodic shift in onset potential indicates more efficient charge separation and reduced recombination in samples anodized at higher voltages, which is consistent with the EIS results showing a decrease in charge transfer resistance (Ge *et al.* 2016; Zhang, 2011).

The stability of the photoanodes was assessed through chronoamperometry measurements at an applied potential of 1.23 V versus RHE under continuous AM 1.5 G illumination for 3 hours. All samples exhibited stable photocurrent response with minimal degradation over the testing period. The TiO_2-30V sample maintained the highest photocurrent throughout the test, with a decrease of less than 5% after 3 hours, demonstrating excellent stability for prolonged operation.

The incident photon-to-current efficiency (IPCE) was measured at an applied potential of 1.23 V versus RHE in the wavelength range of 300-600 nm. All samples showed high IPCE values in the UV region (300-400 nm), corresponding to their strong UV absorption, with the TiO_2-30V sample exhibiting the highest IPCE of approximately 68% at 350 nm.

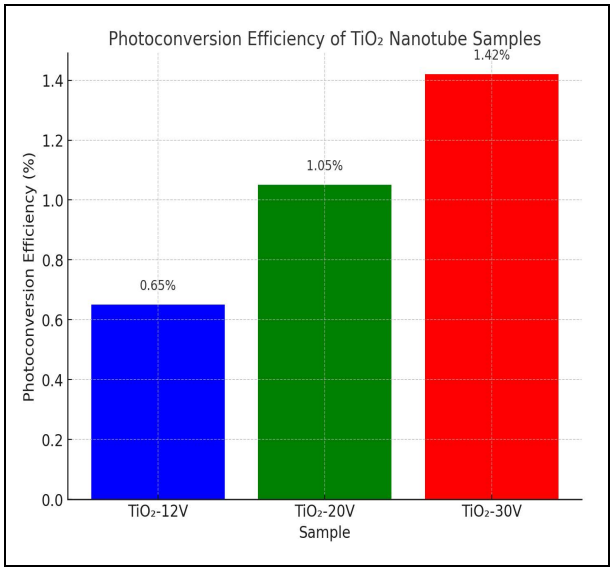


Fig. 4: Photoconversion efficiency of TiO_2 nanotubes

The IPCE values decreased sharply at wavelengths longer than 400 nm, consistent with the limited visible light absorption observed in the UV-Vis spectra. The TiO_2-30V sample showed slightly higher IPCE values in the visible region compared to the other samples, which can be attributed to its marginally reduced bandgap and possibly increased oxygen vacancy concentration.

The photoconversion efficiency (η) was calculated as a function of applied potential using the equation presented in the methods section. All samples exhibited maximum efficiency at approximately 0.4 V versus RHE, where the balance between photocurrent generation and applied voltage is optimized (Gong *et al.* 2010).

The maximum photoconversion efficiencies were 0.65%, 1.05%, and 1.42% for TiO_2-12V, TiO_2-20V, and TiO_2-30V, respectively. The TiO_2-30V sample achieved more than twice the efficiency of the TiO_2-12V sample, further confirming the superior performance of TiO_2 nanotubes fabricated at higher anodization voltages. Fig. 4 shows the maximum photoconversion efficiencies.

The enhanced photoelectrochemical performance of TiO_2-30V can be attributed to a combination of factors. Notably, electrochemical impedance spectroscopy (EIS) measurements revealed a significant reduction in charge transfer resistance, which facilitated more efficient electron transport and interfacial charge transfer. Moreover, the sample exhibited increased donor density and more favorable band alignment, both of which contributed to improved charge separation efficiency. These complementary effects synergistically enhanced the overall photoelectrochemical performance of the TiO_2-30V sample.

These findings highlight the significant impact of anodization voltage on the photoelectrochemical performance of TiO_2 nanotubes, providing valuable insights for optimizing TiO_2 nanotube-based photoanodes for efficient solar water splitting.

6. CONCLUSION

This study investigates the impact of anodization voltage on the electrochemical impedance and photoelectrochemical water splitting performance of TiO_2 nanotubes. Results showed that increasing the anodization voltage significantly enhanced charge transfer kinetics and improved photocurrent density and photoconversion efficiency. Optimized anodization parameters, combined with doping strategies, further boosted visible light absorption and performance. Future work may focus on integrating co-catalysts for hydrogen and oxygen evolution, optimizing processing parameters (electrolyte composition, annealing), and developing scalable fabrication methods for efficient, large-area TiO_2 nanotube photoanodes.

ACKNOWLEDGEMENTS

The authors are thankful to the SRM Institute of Science and Technology, Chennai, TN, India for facilities.

FUNDING

This research received no specific grant from any funding agency in the public, commercial, or not-for-profit sectors.

CONFLICTS OF INTEREST

The authors declare that there is no conflict of interest.

COPYRIGHT

This article is an open-access article distributed under the terms and conditions of the Creative Commons Attribution (CC BY) license (http://creativecommons.org/licenses/by/4.0/).

REFERENCES

David, T. M., Wilson, P., Mahesh, R., Sagayaraj, P., Murugesan, N., Ramesh, C. and Seshadri, H., Photocatalytic water splitting of TiO_2 nanotubes powders prepared via rapid breakdown anodization sensitized with Pt, Pd and Ni nanoparticles, *Mater. Technol.*, 33(4), 288–300(2018). https://doi.org/10.1080/10667857.2018.1433349

Gabov, A. V. and Lizikova, M. S., Hydrogen Energy: Legal Support and International Cooperation, *Her. Russ. Acad. Sci.*, 92, S612–S626(2022). https://doi.org/10.1134/S1019331622130020

Ge, M., Li, Q., Cao, C., Huang, J., Li, S., Zhang, S., Chen, Z., Zhang, K., Deyab, A. S. S. and Lai, Y., One-dimensional TiO_2 Nanotube Photocatalysts for Solar Water Splitting, *Adv. Sci.*, 4(1), 1600152(2016). https://doi.org/10.1002/advs.201600152

Gong, D., Grimes, C. A., Varghese, O. K., Hu, W., Singh, R. S., Chen, Z. and Dickey, E. C., Titanium oxide nanotube arrays prepared by anodic oxidation, *J. Mater. Res.*, 16, 3331-3334(2001a). https://doi.org/10.1557/JMR.2001.0457

Gong, J., Lai, Y. and Lin, C., Electrochemically multi-anodized TiO_2 nanotube arrays for enhancing hydrogen generation by photoelectrocatalytic water splitting, *Electrochimica Acta*, 55(16), 4776–4782(2010b). https://doi.org/10.1016/j.electacta.2010.03.055

Grimes, C. A. and Mor, G. K., Fabrication of TiO_2 Nanotube Arrays by Electrochemical Anodization: Four Synthesis Generations, *TiO2 Nanotube Arrays*, 1–66(2009). https://doi.org/10.1007/978-1-4419-0068-5_1

Kumar, M. P., Jagannathan, R. and Ravichandran, S., Photoelectrochemical System for Unassisted High-Efficiency Water-Splitting Reactions Using N-Doped TiO_2 Nanotubes, *Energy Fuels*, 34(7), 9030–9036(2020). https://doi.org/10.1021/acs.energyfuels.0c00634

Lettieri, S., Pavone, M., Fioravanti, A., Amato, L. S. and Maddalena, P., Charge carrier processes and optical properties in TiO_2 and TiO_2-based heterojunction photocatalysts: A review, *Mater.*, 14(7), 1645(2021). https://doi.org/10.3390/ma14071645

Liu, M. T. H., Zhang, J. and Wang, B., Fabrication of Titanium dioxide nanotube photo-electrodes in different electrolyte mixtures and the impacts on their characteristics and photo-catalytic abilities under visible light, *Pol. J. Chem. Technol*., 19(1), 34–40(2017). https://doi.org/10.1515/pjct-2017-0005

Meena, B., Kumar, M., Kumar, A., Sinha, G. N., Nagumothu, R., Subramanyam, P., Suryakala, D. and Subrahmanyam, C., Integrated p-n Junctions for Efficient Solar Water Splitting upon TiO_2/CdS/$BiSbS_3$ Ternary Hybrids for Improved Hydrogen Evolution and Mechanistic Insight, *Catal.*, 12(10), 1117(2022). https://doi.org/10.3390/catal12101117

Mishra, P. R., Shukla, P. K. and Srivastava, O. N., Study of modular PEC solar cells for photoelectrochemical splitting of water employing nanostructured TiO_2 photoelectrodes, *Int. J. Hydrogen Energy*, 32(12), 1680–1685(2007). https://doi.org/10.1016/j.ijhydene.2006.10.002

Momeni, M. M. and Ghayeb, Y., Fabrication, characterization and photoelectrochemical behavior of Fe-TiO_2 nanotubes composite photoanodes for solar water splitting, *J. Electroanal. Chem*., 751, 43–48(2015). https://doi.org/10.1016/j.jelechem.2015.05.035

Rafique, M., Hajra, S., Irshad, M., Usman, M., Imran, M., Assiri, M. A. and Ashraf, W. M., Hydrogen Production Using TiO_2-Based Photocatalysts: A Comprehensive Review, *ACS Omega,* 8(29), 25640–25648(2023). https://doi.org/10.1021/acsomega.3c00963

Rathod, P. B. and Waghuley, S. A., Synthesis and UV-Vis spectroscopic study of TiO_2 nanoparticles, *Int. J. Nanomanuf*., 11(3–4), 185–193(2015). https://doi.org/10.1504/IJNM.2015.071925

Roy, P., Berger, S. and Schmuki, P., TiO_2 nanotubes: Synthesis and applications, *Angewandte Chem. Int. Edt*., 50(13), 2904–2939(2011). https://doi.org/10.1002/anie.201001374

Schulte, K. L., DeSario, P. A. and Gray, K. A., Effect of crystal phase composition on the reductive and oxidative abilities of TiO_2 nanotubes under UV and visible light, *Appl. Catal. B Environ*., 97(3–4), 354–360(2010). https://doi.org/10.1016/j.apcatb.2010.04.017

Song, H., Luo, S., Huang, H., Deng, B. and Ye, J., Solar-Driven Hydrogen Production: Recent Advances, Challenges, and Future Perspectives, *ACS Energy Lett*., 7(3), 1043–1065(2022). https://doi.org/10.1021/acsenergylett.1c02591

Zakir, O., Idouhli, R., Elyaagoubi, M., Khadiri, M., Aityoub, A., Koumya, Y., Rafqah, S., Abouelfida, A. and Outzourhit, A., Fabrication of TiO_2 Nanotube by Electrochemical Anodization: Toward Photocatalytic Application, *J. Nanomater*., 2020(1), 4745726(2020). https://doi.org/10.1155/2020/4745726

Zhang, J. Z., Metal oxide nanomaterials for solar hydrogen generation from photoelectrochemical water splitting, *MRS Bulletin*, 36(1), 48–55(2011). https://doi.org/10.1557/mrs.2010.9